

# PHYSICAL REVIEW LETTERS

VOLUME 33

1 JULY 1974

NUMBER 1

## End-Point Energy Variations in the Noncharacteristic Radiation Produced by S, Cl, Ar, K, Ca, and Ti Bombardment of Si

G. Bissinger\*†

*Rutgers University, New Brunswick, New Jersey 08903*

and

L. C. Feldman

*Bell Laboratories, Murray Hill, New Jersey 07974*

(Received 1 May 1974)

The noncharacteristic radiation observed in heavy-ion bombardment of Si was investigated with 200-keV  $^{32}\text{S}$ ,  $^{35,37}\text{Cl}$ ,  $^{40}\text{Ar}$ ,  $^{39,41}\text{K}$ ,  $^{40}\text{Ca}$ , and  $^{48}\text{Ti}$  projectiles ( $16 \leq Z \leq 22$ ) on Si. The high-energy tail of the noncharacteristic radiation is observed to shift to higher energies as projectile  $Z$  is increased. The observed end-point energy shifts are in agreement with the interpretation that the radiation arises from the radiative decay of a projectile  $2p$  vacancy in the quasimolecule formed by the projectile and the target atom during the collision.

The noncharacteristic radiation (NCR) extending to  $\approx 1$  keV observed in Ar bombardment of high-purity C, Al, Si, and Fe targets, first reported by Saris, van der Weg, Tawara, and Laubert,<sup>1</sup> has been the subject of intense investigation.<sup>2-4</sup> Using the Fano-Lichten description<sup>5</sup> of heavy-ion collisions, the authors of Ref. 1 interpreted the radiation as arising from the radiative decay of a projectile  $2p$  vacancy in the quasimolecule formed during the collision by the projectile and an atom (either implanted Ar<sup>1</sup> or the target itself<sup>4</sup>). The energy of the emitted radiation then depends on the internuclear separation at the time the vacancy is filled, and on the particular combination of projectile and target atom. The maximum energy (end-point energy) occurs when the vacancy decays at the distance of closest approach,  $\rho_{\text{min}}$ ; for zero internuclear separation, the energy is just that of the united-atom  $L$  x ray, in the absence of additional velocity-broadening effects. Experimental reports have now confirmed<sup>2,3</sup> the original observation of the

NCR, demonstrated that the NCR is a broad photon energy distribution whose low-energy cutoff (as observed in previous experiments) was due to detector-window transmission effects,<sup>4</sup> and studied the projectile-energy dependence of the NCR in the Ar+Si system<sup>1</sup> and in a similar process in the C+C system.<sup>6</sup>

Since the radiation is expected to be a continuum, the end-point energy is a distinctive characteristic of the proposed model. However, for a variety of reasons (e.g., collision broadening and experimental determination of end-point energies), the absolute value of the end-point energy is rather poorly defined. In this Letter we report the first systematic investigation of the end-point energy dependence on  $Z_1$ , the atomic number of the projectile. As a result of using a set of projectiles with closely spaced atomic numbers, we can make use of the end-point energy differences, thus reducing much of the ambiguity in the direct comparison of experimental and theoretical end-point energies. This sensitive and

explicit test of the explanation of the source of the NCR confirms the general model given in Ref. 1.

The experiment utilized mass-analyzed 200-keV beams of  $^{32}\text{S}^+$ ,  $^{35,37}\text{Cl}^+$ ,  $^{40}\text{Ar}^+$ ,  $^{39,41}\text{K}^+$ ,  $^{40}\text{Ca}^+$ , and  $^{48}\text{Ti}^+$ . The target chamber and associated equipment have been described elsewhere.<sup>4</sup> Dose-related effects were kept to a minimum by keeping all doses below  $10^{16}$  atoms/cm<sup>2</sup> where projectile-implanted-projectile collision contributions to the NCR first become noticeable,<sup>4</sup> and also by changing the target position frequently. A Si(Li) detector with a 12.7- $\mu\text{m}$  Be window was used to detect the x radiation; count rates were kept below 300 counts/sec to reduce pileup and gain shifts.

Thick Si targets were bombarded with the various projectiles; the spectra collected for  $^{32}\text{S}$  and  $^{48}\text{Ti}$  projectiles are shown in Fig. 1(a) and clearly demonstrate the upward shift on the high-energy side of the NCR for the higher- $Z$  projectile. Intermediate shifts are observed for the other projectiles, depending only on  $Z_1$ . To demonstrate that the projectile mass does not affect the end-point energy, the spectra obtained for two isotopes of Cl are shown in Fig. 1(b). No variation in the end-point energy was observed for the two K isotopes either (not shown).

Following the procedure in Ref. 6, we defined an end-point energy as the intersection of the line drawn tangent to the high-energy side at the half-maximum and the abscissa on a linear scale. Since all the NCR spectra had similar shapes on the high-energy side, this approach does not have as large a systematic error as the determination of end-point energies for varying projectile ener-

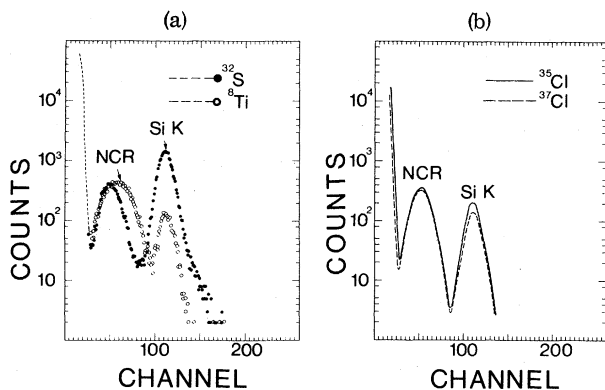


FIG. 1. (a) 200-keV  $^{32}\text{S}$  and  $^{48}\text{Ti}$  on thick Si. Spectra are shifted vertically to overlap noncharacteristic radiation near 1 keV. (b) 200-keV  $^{35}\text{Cl}$  and  $^{37}\text{Cl}$  on thick Si. Spectra have been normalized to collected charge.

gy does,<sup>1,6,7</sup> because of the variation in peak shape observed in the latter. However, the variation in the detector-window transmission is still important in this energy region, ranging from about 25 to 45% for 1 to 1.5 keV. This transmission variation has the effect of increasing the end-point energy determined as described above, and is most important for the lowest- $Z$  projectiles. It also reduces the end-point energy differences between spectra for adjacent  $Z_1$ , particularly for lower  $Z$ . The experimental end-point energies are shown in Fig. 2(a), and demonstrate the monotonic increase in end-point energy as projectile  $Z$  increases. The errors shown in Fig. 2(a) represent an estimate of random errors only and do not include systematic errors due to the following: (i) detector resolution (approximately constant over our energy range), (ii) Si  $K$  tail (which is small and makes approximately the same contribution for all projectiles since for the lower- $Z$  projectiles the Si  $K$  is more intense but relatively far from the half-maximum of the NCR), and (iii) NCR shape variations on the high-energy side and detector-window (and detector Si dead-layer) transmission effects. The latter error is expected to be the dominant one for the lower- $Z$  projectiles (if one disregards the systematic error inherent in our method of determining end-point energies).

As a means of removing some of the systematic errors, experimental end-point energy differences were extracted and normalized to the maximum possible differences associated with the  $2p$  binding energy in the united atom. First, we define

$$C_i(\rho_{\min}) \equiv E_i/E_i(2p),$$

where  $E_i$  is the binding energy of the  $2p\pi$  level

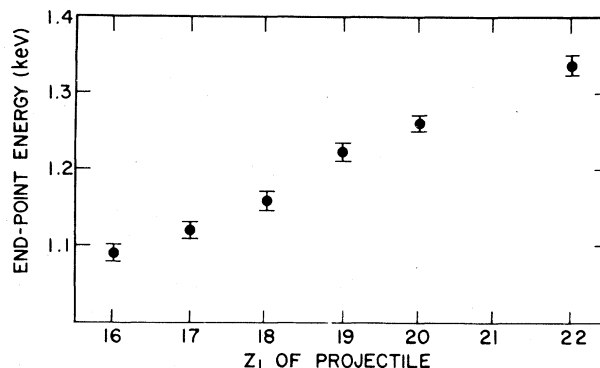


FIG. 2. End-point energies for S, Cl, Ar, K, Ca, and Ti on thick Si.

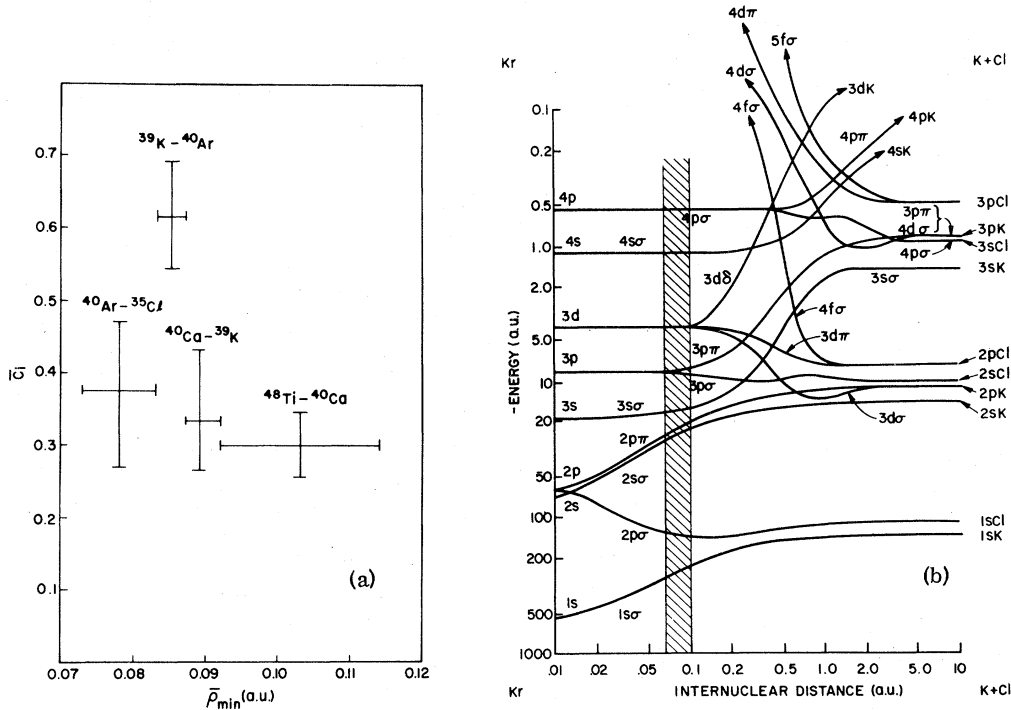


FIG. 3. (a)  $\bar{C}_i(\rho_{\min})$  as a function of  $\rho_{\min}$ . The horizontal flag on a datum point is derived from the two distances of closest approach associated with the two projectiles. (b) the  $\text{K} + \text{Cl}$  correlation diagram (from Ref. 8) indicating the region of internuclear separation measured.

at  $\rho_{\min}$  for the projectile  $Z=i$  and  $Z=14$  system, and  $E_i(2p)$  is the  $2p$  binding energy of the united atom formed by  $Z=i$  and  $Z=14$ , i.e., at  $\rho_{\min}=0$ . Furthermore we assume

$$C_i \cong C_{i+1} \equiv \bar{C}_i;$$

that is, we assume that the *shape* of the molecular orbital (MO) diagrams does not vary greatly over the small differences in  $\rho_{\min}$  and  $Z$  associated with two neighboring projectiles. We then calculate

$$\frac{E_{i+1}(\text{exp}) - E_i(\text{exp})}{E_{i+1}(2p) - E_i(2p)} = \bar{C}_i(\rho_{\min}),$$

where  $\bar{C}_i$  is a measure of the binding energy of the united-atom  $2p$  level at  $\rho_{\min}$ , and  $E_i(\text{exp})$  is the experimentally determined cutoff energy. The large advantage in this formulation is the use of the difference of two experimental cutoffs, thus canceling many uncertainties in the end-point energy definition. Figure 3(a) shows the results of this analysis and indicates that  $\bar{C}_i \cong 0.4$  with an indication of a trend to higher  $\bar{C}_i$  with smaller  $\rho_{\min}$  (the S-Cl difference has been omitted because of the uncertainty in the window correction). The horizontal flag on a datum point is determined by the two distances of closest ap-

proach associated with the two projectiles, while the vertical error bar is estimated from the reproducibility of the cutoff energy. The Ar-Cl point may be low because of the large effect of the Be window on the Cl+Si distribution. The formula for  $\bar{C}_i(\rho_{\min})$  and the assumptions in its derivation have been extended and applied to obtain the Ca-Ti point where the atomic number varies by 2.

Figure 3(b) shows the MO diagram for the  $\text{K} + \text{Cl}$  system ( $Z_1 + Z_2 = 36$ )<sup>8</sup> corresponding to a united atom which is the same as the Ti+Si system described here. We also note that the order of the tightly bound levels is the same for the two systems. Indicated in the diagram is the region of internuclear separation explored in this study; in particular, for an internuclear distance of 0.1 a.u. the diagram yields  $C_i = 0.33$ , while the experimental result derived from the  $^{48}\text{Ti}-^{40}\text{Ca}$  measurements is 0.30. If the present experiments were systematically carried to higher energy, the minimum internuclear separation would decrease and the experimental end-point energy differences would presumably lead to  $C_i$  approaching 1. This seems to be a way of experimentally mapping out the MO diagram. It would, of course,

be useful to have more exact calculations for the particular systems studied here, as well as extending these experiments to a broader range of  $\rho$ .

The yield of Si  $K$  x rays present in the spectra of Fig. 1 will be discussed in detail elsewhere.<sup>9</sup> Additional experiments have shown that at the energy used in the present study, they do not primarily arise from a  $2p$  vacancy transfer to the Si  $K$  level but from recoil Si-Si collisions as has been shown for Ar-Al.<sup>10</sup> At sufficiently higher energies, however, the minimum internuclear separation is small enough to make vacancy transfer to the  $1s$  level of Si the dominant mechanism for Si  $K$  x-ray production.

The present results strongly support the original interpretation of the NCR. The systematic shift with  $Z_1$  is in accord with expectation and the quantitative magnitude of the shift is quite consistent with the range of minimum internuclear separations produced in 200-keV collisions.

We would like to acknowledge useful discussions with J. S. Briggs, W. L. Brown, and J. R. Macdonald and the technical aid of J. W. Rodgers.

\*Work supported in part by the National Science Foundation.

†Present address: Physics Department, East Carolina University, Greenville, N. C. 27834.

<sup>1</sup>F. W. Saris, W. F. van der Weg, H. Tawara, and R. Laubert, Phys. Rev. Lett. **28**, 717 (1972).

<sup>2</sup>J. Macek, J. A. Cairns, and J. S. Briggs, Phys. Rev. Lett. **28**, 1298 (1972).

<sup>3</sup>J. R. Macdonald and M. D. Brown, Phys. Rev. Lett. **29**, 4 (1972).

<sup>4</sup>G. Bissinger and L. C. Feldman, Phys. Rev. A **8**, 1624 (1973).

<sup>5</sup>U. Fano and W. Lichten, Phys. Rev. Lett. **14**, 627 (1965); W. Lichten, Phys. Rev. **164**, 131 (1967).

<sup>6</sup>J. R. Macdonald, M. D. Brown, and T. Chiao, Phys. Rev. Lett. **30**, 471 (1973).

<sup>7</sup>F. W. Saris *et al.*, in *Proceedings of the International Conference on Inner-Shell Ionization Phenomena and Future Applications*, Atlanta, Georgia, 1972, edited by R. W. Fink, J. T. Manson, I. M. Pálms, and R. V. Rao, CONF-720404 (U.S. Atomic Energy Commission, Oak Ridge, Tenn., 1973).

<sup>8</sup>M. Barat and W. Lichten, Phys. Rev. A **6**, 211 (1973).

<sup>9</sup>L. C. Feldman, G. Bissinger, and J. S. Briggs, to be published.

<sup>10</sup>K. Taulbjerg, B. Fastrup, and E. Laegsgaard, Phys. Rev. A **8**, 1814 (1973).

## New Method for Lamb-Shift Measurements\*

A. van Wijngaarden, G. W. F. Drake,† and P. S. Farago‡

*Department of Physics, University of Windsor, Windsor, Ontario, N9B 3P4, Canada*

(Received 7 May 1974)

The anisotropy in the quenching radiation of H atoms in the metastable  $2s$  state has been studied with the aim of developing a new method for Lamb-shift measurements in hydrogenic ions. The extrapolated value of the anisotropy at zero field strength is  $0.1392 \pm 0.0015$ , in good agreement with the theoretical prediction  $0.13904$  based on the accepted value of the Lamb shift and a consideration of hyperfine coupling effects. Our anisotropy corresponds to a Lamb shift of  $1059 \pm 13$  MHz.

The comparison of Lamb-shift measurements in hydrogen and the hydrogenic ions with theoretical calculations remains one of the important tests of quantum electrodynamics.<sup>1</sup> The Lamb shifts in H,<sup>2</sup> D,<sup>3</sup> He<sup>+</sup>,<sup>4</sup> and Li<sup>2+</sup><sup>5</sup> are now accurately known from experiments using microwave resonance techniques, but no technique of comparable accuracy is available for the heavier ions. A much less accurate method based on a measurement of the quenching rate of the metastable  $2s_{1/2}$  state in an electric field has been applied to Li<sup>2+</sup>,<sup>6</sup> C<sup>5+</sup>,<sup>7</sup> and O<sup>7+</sup>,<sup>8,9</sup> but the results are far from matching the accuracy of the calculations of Erickson.<sup>10</sup> We report in this Letter some preliminary results for hydrogen which in-

dicates that a method recently suggested by Drake and Grimley<sup>11</sup> is capable of an accuracy at least as good as obtained by the quenching-rate technique. In addition, the results resolve a possible discrepancy between theory and experiment found by Ott, Kauppila, and Fite<sup>12</sup> in their measurement of the polarization of the quenching radiation.

Fite, Kauppila, and Ott<sup>12</sup> and Casalese and Gerjuoy<sup>13</sup> first pointed out that the quenching radiation is polarized, but it was not appreciated until recently that in addition the radiation summed over both polarizations is anisotropic.<sup>11</sup> Since the anisotropy is approximately proportional to the Lamb shift, a measurement of the total num-